Contrib Mineral Petrol 75, 179–186 (1980)

Contributions to Mineralogy and Petrology

Lawsonite Zone Blueschists and a Sodic Amphibole Producing Reaction in the Tavşanlı Region, Northwest Turkey

A.I. Okay*

Department of Earth Sciences, Downing Place, Cambridge CB2 3EW, England

Abstract. The petrology and mineralogy of lawsonite zone metabasites have been studied northeast of town of Tavşanlı, NW Turkey. In the field the metabasites are characteristically green and lack foliation; the essential mineral assemblage being sodic pyroxene + lawsonite + chlorite + quartz ± sodic amphibole. Sodic pyroxene of aegirine-jadeite composition occurs as pseudomorphs after magmatic augite. Lawsonite and chlorite are the other two dominant minerals. Sodic amphibole forms progressively from a reaction between sodic pyroxene, chlorite and quartz, and an isograd representing the first abundant occurrence of sodic amphibole in basic rocks has been mapped. The widespread occurrence of sodic pyroxene pseudomorphs in other blueschist terrains indicates that the inferred sodic amphibole producing reaction is of general significance for blueschist metabasites.

The conversion of greenstones with the assemblage albite + chlorite + actinolite directly into glaucophane-lawsonite blueschists without any intervening lawsonite zone illustrates the influence of the initial mineral assemblage on the reaction path.

Introduction

The Northwest Turkish blueschist belt extends 250 km in an east-west direction flanking the northern margins of the ultrabasic massifs in the İzmir-Ankara Zone (Okay 1980a, Fig. 1). The dominant rock types throughout the belt are basic volcanic rocks, pyroclastics, cherts and shales. The volcanics and tuffs are repeatedly intercalated with pelagic sediments indicating that volcanism was contemporaneous with sedimentation. The metamorphic grade shows a general increase northwards away from the peridotite massifs from incipient high pressure metamorphism to glaucophane-lawsonite or glaucophane-epidote zone blueschists. The increase in metamorphic grade takes place over a distance of 10–20 km. A section across this peridotite/blueschist belt has been mapped northeast of the district of Tavşanlı (Okay 1980a, Fig. 1). Here an imbricate tectonic zone of spilite-chert-serpentinite association with occasional slices of greenschists, forms a 2–3 km wide rim around the large harzburgite massifs. The spilites of this zone show effects of an incipient high-pressure metamorphism and metasomatism (Okay, in preparation). This schuppen zone is succeeded along major thrust faults by the lawsonite zone blueschists, which pass with the development of sodic amphibole to fully recrystallised and often schistose glaucophane-lawsonite zone blueschists (Okay 1980a). This paper deals with the lawsonite zone blueschists around the village of Ketenlik, south of the area shown in Fig. 1 of Okay (1980a).

Rock Types and Petrography

The rock types in the area include basic volcanics, cherts, shales, serpentinite, gabbro and greywacke. Metabasites, which are the most common lithology, form massive green dolerites, pyroclastics and lava flows. In the field the basic volcanic rocks are green, appear unmetamorphosed and show no penetrative deformation. The only sign of blueschist metamorphism is rare blue stringers of sodic amphibole along shear planes. However, under the microscope the igneous mineralogy is seen to be completely reconstituted while the igneous texture is preserved. Augite is pseudomorphed by sodic pyroxene (cf., Carpenter and Okay 1978), while the rest of the rock consists of an assemblage of lawsonite-quartz-chlorite-leucoxene (Fig. 1). In some rocks large plagioclase crystals have been pseudomorphed by an assemblage of lawsonite-quartz-chlorite (cf., Çoğulu 1967, Photo 20). Except for the general absence of pumpellyite, the lawsonite zone metabasites of the Tavşanlı area closely resemble the Type II metabasites of the Franciscan (Coleman and Lee 1963). The common mineral assemblages in the lawsonite zone metabasites are:

lawsonite + sodic pyroxene + chlorite + quartz + leucoxene
± phengite ± sodic amphibole.

---

* *Present address:* Temel Araştırmalar, Mineral Research and Exploration Institute (MTA), Ankara, Turkey

0010/7999/80/0075/0179/$01.60

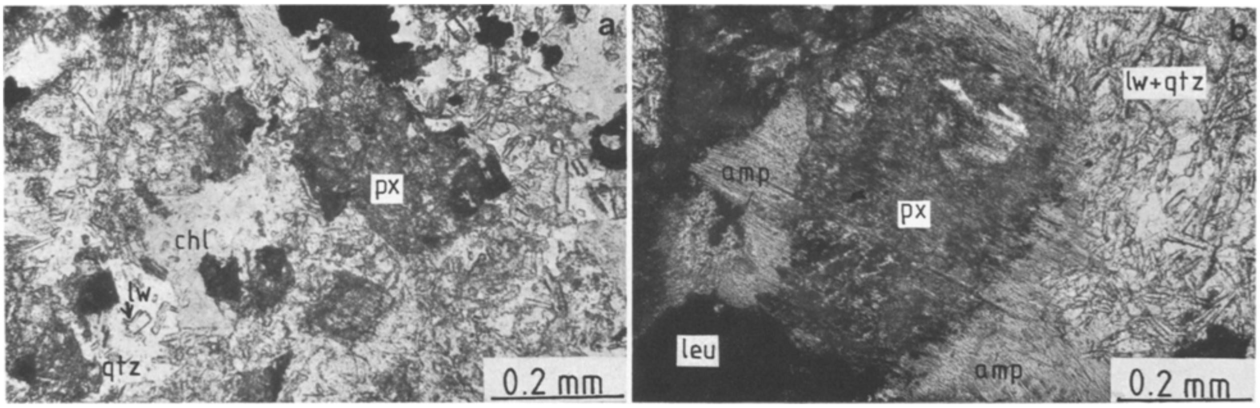

Fig. 1a and b. Photomicrographs of lawsonite zone metabasites from the Tavşanlı region: **a** Sodic pyroxene pseudomorphs (*px*) after augite set on a chlorite (*chl*)+lawsonite (*lw*)+quartz (*qtz*)+matrix; leucoxene is after titanomagnetite. **b** Coarse grained metadolerite (K54) with sodic pyroxene pseudomorphs (*px*) rimmed and partially replaced by sodic amphibole (*amp*). The groundmass consists of lawsonite and quartz. Sodic pyroxene has irregular quartz inclusions

Sodix pyroxene, lawsonite and chlorite occur in roughly equal proportions, and together constitute approximately 80 modal per cent of the rock (Table 1). Leucoxene and quartz usually make up less than 10%. Sodic amphibole occurs either as thin rims around sodic pyroxene pseudomorphs (Fig. 1b) or as idioblastic crystals growing over a fine-grained sodic pyroxene-chlorite matrix. Sodic amphibole, when present, generally does not constitute more than 10% of the metabasite in the lawsonite zone. A few grains of pyrite or magnetite were noted from about one quarter of the specimens. In general carbonate minerals are rare, but small amounts of aragonite, partially inverted to calcite, occur in the groundmass of five specimens. Albite is absent. Measured modes of six analysed metabasites based on over 1,000 point counts are given in Table 1.

Veins are not very abundant in the lawsonite zone metabasites; the vein minerals include quartz (in 17 samples out of 40), calcite (in 4), aragonite (in 2), chlorite (in 2), lawsonite (in 2), and sodic pyroxene (in 1).

Red cherts, which are intercalated with the metabasites, are poorly recrystallised and retain their sedimentary features. Ultrabasic rocks occur as small lenses within the lawsonite zone sequence. They are completely serpentinised and consist of antigorite (as determined by its XRD patterns cf. Whittaker and Zussman 1956) with minor chlorite, brucite, tremolite, disseminated magnetite and relict spinel. Irregular veins and granules of andradite garnet ($Ca_{2.98}Mn_{0.02}Fe^{3+}_{1.84}Al_{0.11}Ti_{0.04}Si_3O_{12}$) are commonly present in these serpentinites.

Rare volcanogenic greywackes retain their sedimentary textures. However, albite clasts have been replaced by prismatic bundles of jadeite and quartz; the quartz grains show incipient recrystallisation.

Table 1. Measured modes of analysed lawsonite zone metabasites

	K54	K625	K627	K761	K769	K782	K856*
Lawsonite	32.1	20.2	44.6	23.8	29.7	15.0	×
Chlorite	8.9	27.5	1.1	18.6	25.6	26.7	×
Sodic pyroxene	26.1	33.3	26.2	42.0	22.1	45.2	×[a]
Sodic amphibole	13.7	–	20.4	–	–	0.9	–
Quartz	13.6	14.1	0.2	4.1	4.0	0.1	–
Leucoxene	3.1	4.4	5.4	11.2	11.1	10.1	×
Phengite	2.5	–	1.7	–	7.5	1.0	–
Pyrite	–	–	–	0.3	–	tr	×
Magnetite	–	0.5	–	–	–	–	–
Relict augite	–	–	0.4	–	–	1.0	×
	100.0	100.0	100.0	100.0	100.0	100.0	

* Too fine-grained for modal counting

[a] Jadeitic pyroxene

Method

Mineral compositions were determined for twelve elements (Na, Ca, K, Fe, Mg, Mn, V, Ni, Cr, Ti, Al, Si) using an energy dispersive electronprobe with a Harwell Si(Li) detector and pulse processor. The correction procedures are given by Sweatman and Long (1969). The method for estimating ferric ion in sodic pyroxene and sodic amphibole is given in earlier papers (Okay 1978, 1980b respectively).

Mineralogy

Sodic Pyroxene

All sodic pyroxenes in the metabasites are pseudomorphs after augite. In the 40 samples that were examined, sodic pyroxene was never found to have nucleated independently. In the great majority of the specimens sodic pyroxene forms apple-green crystals, which are often turbid as a result of small leucoxene inclusions (Fig. 1). Such sodic pyroxenes are aegirine-jadeites with high acmite components (>40%, Fig. 2, Table 2). In four specimens augites are partially or completely replaced by jadeitic pyroxene. In two of these cases jadeite and acmitic pyroxene have replaced different grains in the same section, or even different parts of the same grain. The compositions of the jadeitic pyroxenes from one of these metabasites are plotted in Fig. 2. Omphacite, which occurs in some Type II metabasites from the Franciscan (Essene and Fyfe 1967, Figs. 12 and 13; Brown and Bradshaw 1980, Fig. 3) is not found in the Tavşanlı area.

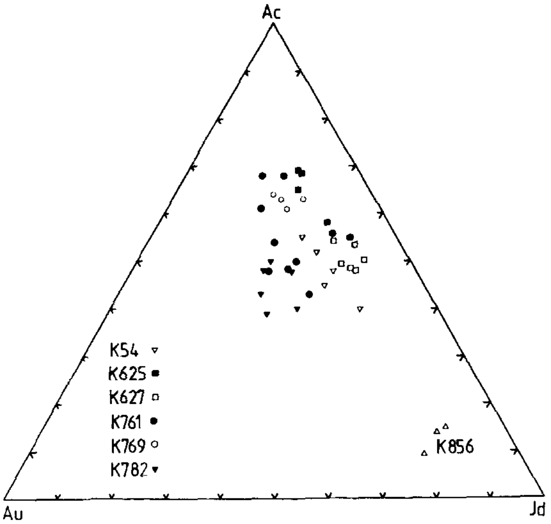

Fig. 2. Sodic pyroxene compositions from the lawsonite zone metabasites plotted on the acmite-jadeite-augite diagram

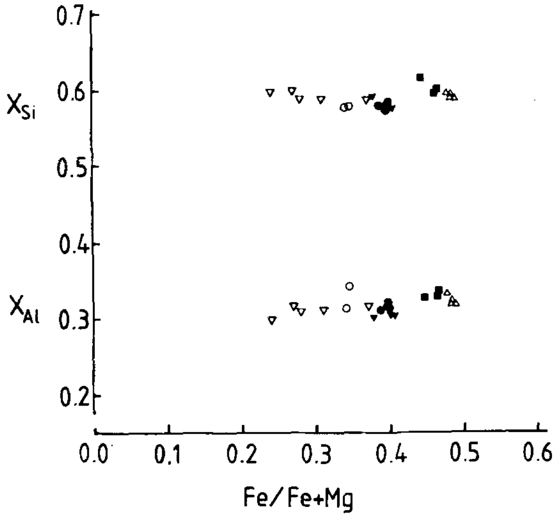

Fig. 3. Chlorite compositions from the lawsonite zone metabasites plotted in terms of their Fe/Fe+Mg, Si/Si+Al and Al/Al+Fe+Mg ratios. Symbols as in Fig. 2

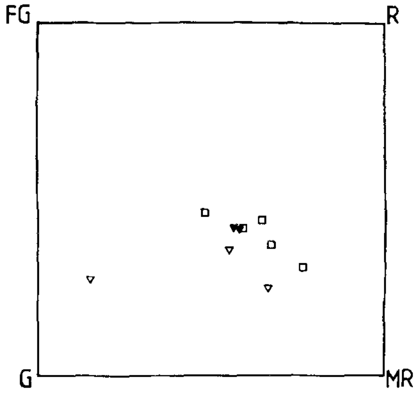

Fig. 4. Sodic amphibole compositions from the lawsonite zone metabasites plotted on the Miyashiro diagram. Symbols as in Fig. 2. *G* glaucophane; *FG* ferroglaucophane; *R* riebeckite; *MR* magnesioriebeckite

Chlorite

In contrast to the glaucophane-lawsonite zone, chlorite is abundant in the lawsonite zone metabasites. However, it is less well recrystallised and often has appreciable K_2O and CaO contents (Table 2). Chlorite compositions from six metabasites are plotted in Fig. 3 and four chlorite analyses are shown in Table 2. Chlorites show a wide range of ferromagnesian ratios ($X_{Fe} = 0.2$–0.5) and a restricted Al/Al+Fe+Mg ratio (0.30–0.34). There is no appreciable compositional difference between the glaucophane-lawsonite and lawsonite zone chlorites.

Lawsonite

Lawsonite invariably forms small tabular crystals with prominent (101) faces. Compositionally it is very uniform and closely approximates the ideal structural formula $CaAl_2Si_2O_7H_2O(OH)_2$.

Sodic Amphibole

Sodic amphiboles, which are texturally replacing sodic pyroxenes (cf., Fig. 1b) tend to be compositionally inhomogeneous with Ca-rich patches. This apparently has arisen from the difficulty of diffusing calcium atoms away from the sodic pyroxene through the mantling sodic amphibole. Idioblastic sodic amphiboles growing over the chlorite-sodic pyroxene matrix are uniformly homogeneous and sodium-rich ($Na/Na+Ca > 90\%$). Sodic amphibole compositions from three metabasites are plotted on the Miyashiro diagram in Fig. 4 and two of the analyses are given in Table 2.

Phengite

Phengite is much rarer in the lawsonite zone metabasites than in the corresponding higher grade glaucophane-lawsonite zone metabasites. It forms feathery elongate crystals closely associated and often intergrown with chlorite. Its formation is related to the recrystallisation of relatively potassium-rich microgranular chlorite to potassium-poor coarser chlorite. The few analysed phengites do not have any measurable paragonite or margarite components (Table 2).

Leucoxene

Leucoxene is a constant accessory mineral in the metabasites. It forms diffuse semiopaque pseudomorphous after titanomagnetite or ilmenite. It has a nonstoichiometric and variable composition with sphene as the dominant mineral (Table 2).

Sodic Amphibole Isograd

The passage from green, massive lawsonite-chlorite-sodic pyroxene rocks to blue, often schistose glaucophane-lawsonite metabasites is gradual. The more

Table 2. Representative mineral analyses

	Sodic pyroxene					Chlorite				Sodic amphibole		Phengite	Leucoxene	
	K625	K761	K627	K782	K856	K625		K769		K54	K627	K782	K761	K54
SiO_2	53.92	53.67	55.67	54.26	58.40	29.55	29.19	28.68	29.05	59.48	56.75	52.43	30.00	29.78
TiO_2	0.25	0.40	1.05	0.14	0.14	0.00	0.00	0.00	0.00	0.43	0.17	0.00	25.95	39.05
Al_2O_3	5.02	5.16	9.66	6.60	18.08	16.70	16.79	17.87	18.05	10.23	5.99	21.73	6.42	2.42
FeO^a	21.19	18.47	15.77	13.25	5.94	21.64	22.51	18.77	16.75	9.82	19.47	4.51	7.79	2.23
MgO	1.41	3.08	1.46	4.82	1.43	13.95	14.60	20.48	17.81	10.80	7.69	4.63	6.12	1.42
MnO	0.00	0.00	0.00	0.00	0.00	0.49	0.77	0.56	0.54	0.19	0.19	0.00	0.15	0.00
CaO	2.99	6.05	2.37	9.10	2.67	0.39	0.22	0.13	0.28	0.44	0.69	0.00	19.45	23.60
Na_2O	12.99	10.65	12.73	9.46	13.32	0.00	0.00	0.00	0.00	7.78	7.02	0.00	0.00	0.00
K_2O	0.00	0.00	0.00	0.00	0.00	1.47	0.49	0.09	0.98	0.00	0.00	10.46	0.00	0.00
Total	97.77	97.48	98.71	97.63	99.98	84.19	84.57	86.58	83.46	99.17	97.97	93.76	95.88	98.50

[a] Total iron as FeO

	Number of cations per													
	6 oxygens					28 oxygens				23 O		22 O	5 oxygens	
Si	1.99	2.00	2.01	2.00	2.02	6.40	6.29	5.91	6.16	7.97	8.01	7.18	1.02	0.98
Al^4	0.01	0.00	0.00	0.00	0.00	1.60	1.71	2.09	1.84	0.03	0.00	0.82	0.26	0.09
Al^6	0.21	0.23	0.41	0.29	0.74	2.66	2.56	2.25	2.68	1.59	1.00	2.69		
Ti	0.01	0.01	0.03	0.00	0.00	0.00	0.00	0.00	0.00	0.04	0.02	0.00	0.66	0.97
Fe^{3+}	0.65	0.54	0.48	0.39	0.15	3.92	4.06	3.24	2.97	0.28	0.91	0.52	0.22	0.06
Fe^{2+}	0.00	0.03	0.00	0.02	0.02					0.82	1.39			
Mg	0.08	0.17	0.08	0.26	0.07	4.50	4.69	6.29	5.63	2.16	1.62	0.95	0.31	0.07
Mn	0.00	0.00	0.00	0.00	0.00	0.09	0.14	0.10	0.10	0.02	0.02	0.00	0.01	0.01
	0.95	0.98	1.00	0.96	0.98					4.91	4.96	4.16		
Ca	0.12	0.24	0.09	0.36	0.10	0.09	0.05	0.03	0.06	0.06	0.10	0.00	0.71	0.83
Na	0.93	0.77	0.89	0.68	0.89	0.00	0.00	0.00	0.00	2.02	1.92	0.00	0.00	0.00
K	0.00	0.00	0.00	0.00	0.00	0.41	0.13	0.02	0.27	0.00	0.00	1.83	0.00	0.00
	1.05	1.01	0.98	1.04	0.99	19.67	19.63	19.93	19.71	2.08	2.02	1.83	3.19	3.01
Jd	22	23	41	29	74									
Ac	65	54	48	39	15									
Au	13	23	11	32	11									

fissile volcanic shales and tuffs obtain a blue colour before the coarser dolerites and basalts which stand out as green massive boundinaged blocks amidst the strongly schistose blue metashales. The sodic amphibole isograd is mapped in these massive basalts and dolerites. ("Isograd" is used here purely in the descriptive sense – e.g., the first abundant appearance of sodic amphibole in massive metabasites).

The passage from lawsonite zone to glaucophane-lawsonite zone occurs within 50 m in the village of Ketenlik. The change in mineral assemblage was observed in two banded tuff specimens collected from within 50 m of each other. K507/2 is green and shows a well-marked banding, and consists of elongated, yellowish-green sodic pyroxene, and chlorite + lawsonite bands with minor quartz but no sodic amphibole. K507/1 collected 50 m to the south is blue and schistose, and consists of over 40 modal per cent sodic amphibole and abundant lawsonite. Sodic pyroxene has largely resorbed or concentrated along certain bands.

Figure 5 is a geological map of the Ketenlik area, NW Turkey showing the sample locations of the basic igneous rocks. Locations of metabasites with the essential mineral assemblage lawsonite + chlorite + sodic pyroxene (after augite) are shown by filled circles. Half-filled circles indicate specimens which also contain minor amounts of sodic amphibole. Metabasite locations with the essential mineral assemblage of sodic amphibole + lawsonite are shown by open circles. The isograd closely follows the tectonic boundaries of the incipiently metamorphosed spilite-chert-serpentinite complex (Yeniköy Group).

The formation of sodic amphibole is generally contemporaneous with the penetrative deformation in the blueschists. In the lawsonite zone, sodic amphibole occurs only along the shear planes in the green massive metabasites, where it forms thin blue scales.

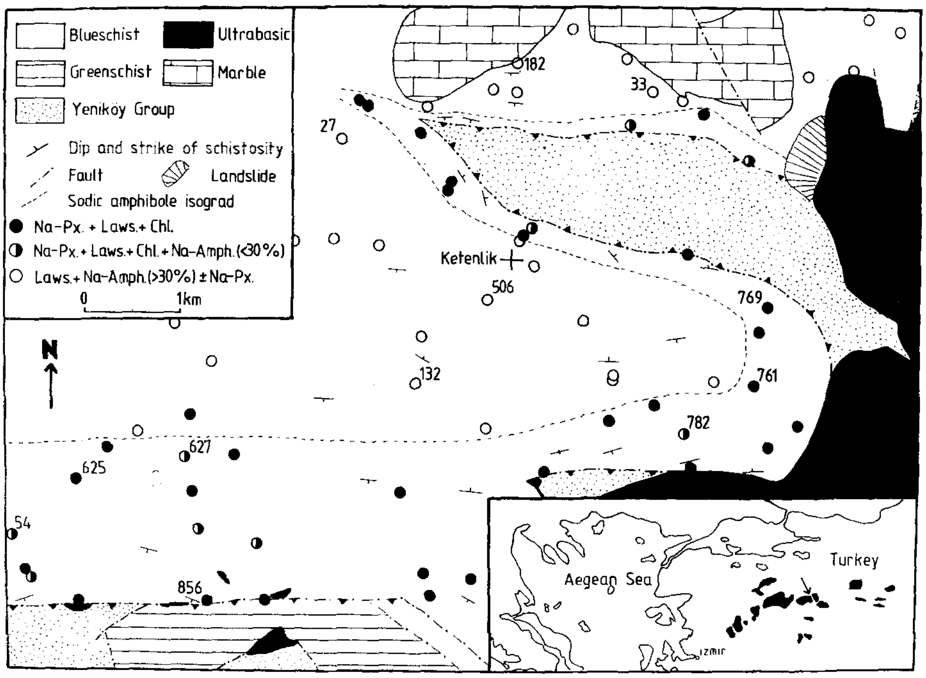

Fig. 5. Geological map of the Ketenlik area showing the sample locations and the sodic amphibole isograd. Yeniköy Group consists of an incipiently metamorphosed and metasomatised spilite-chert-serpentinite complex. The *inset* shows the major peridotite occurrences in Western Turkey

With increasing deformation sodic amphibole grows parallel to the schistosity wrapping around rotated sodic pyroxene and lawsonite crystals. The typical mineral assemblage in the glaucophane-lawsonite zone metabasites is "sodic amphibole+lawsonite± sodic pyroxene±chlorite+sphene+phengite". The ghost igneous texture, which is so well preserved in the lawsonite zone metabasites, is completely obliterated with the development of a schistose metamorphic fabric. Cherts which are clearly recognizable as such in the lawsonite zone, lose their distinct red colour, and form banded, schistose metaquartzites. These rocks are described in detail in the previous paper (Okay 1980a).

Sodic Amphibole Producing Reaction in the Metabasites

The reaction textures between sodic pyroxene and sodic amphibole, as well as the drastic decrease in the modal amounts of chlorite and sodic pyroxene in the glaucophane-lawsonite zone metabasites, indicate that the formation of sodic amphibole is related to a reaction involving chlorite and sodic pyroxene.

In quartz-bearing rocks, the minerals sodic pyroxene, sodic amphibole, chlorite and lawsonite can be described in the six component system $Na_2O-CaO-FeO-MgO-Al_2O_3-Fe_2O_3$. The relationship between sodic pyroxene and sodic amphibole in this system can be shown in a ternary phase projection with Na, Al and Fe^{3+} at its apices (NAF3), involving projections from lawsonite for Ca and from chlorite for Fe^{2+}, Mg (Fig. 6). Both lawsonite and chlorite are stable and ubiquitous on both sides of the isograd. The composition of chlorite used in the projection is $(Fe^{2+}, Mg)_{4.80}Al_{2.20}Si_{2.95}O_{10}(OH)_8$, typical of blueschist chlorites. The variation of $Al/Fe^{2+}+Mg$ of chlorites in different rocks is slight (Fig. 3) and

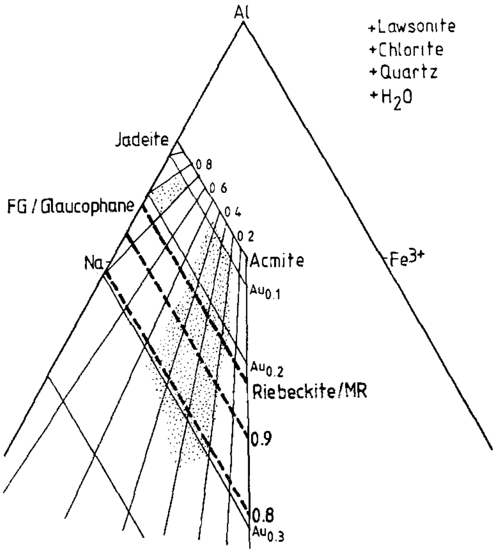

Fig. 6. NAF3 projection of sodic pyroxene and sodic amphibole compositions from lawsonite, chlorite, quartz, and H_2O. The jadeite and augite contents of sodic pyroxenes, and the Na/Na+Ca ratios of sodic amphiboles (*thick dashed lines*) are indicated. The observed sodic pyroxene compositional field from the lawsonite zone metabasites is stippled

there is no appreciable difference in the Al/Al+Fe+Mg ratios of chlorites from lawsonite and glaucophane-lawsonite zones. The algebraic procedure used for projecting phases is that given by Greenwood (1975).

Only Ca-poor sodic pyroxenes can be represented (approx. $<Au_{35}$) in the NAF3 diagram as the more calcic members have negative projection points. However, this is not a problem as all analysed sodic pyroxenes from metabasites have low augite contents ($<Au_{30}$). The compositional range of sodic pyroxenes from metabasites is shown stippled in the NAF3 diagram in Fig. 6. Sodic amphibole compositions down to $Na/Na+Ca=0.8$ (as observed in metabasites) are indicated by dashed lines.

The most important feature revealed by the NAF3 diagram in Fig. 6 is the superposition of the sodic amphibole and sodic pyroxene fields. This indicates that sodic pyroxenes, with compositions corresponding to the sodic amphibole field in the NAF3 diagram, are not stable with sodic amphibole in the presence of quartz, lawsonite and chlorite under divariant conditions. For sodic pyroxenes with compositions lying outside the sodic amphibole field in the NAF3 diagram ($Au<0.2$ or $Au>0.3$), the sodic amphibole producing reaction would be a continuous one, producing sodic pyroxenes further enriched ($>Au_{0.3}$), or depleted ($<Au_{0.2}$) in augite component than the initial composition (depending on which side of the sodic amphibole field they lie). As pointed out by Brown and Bradshaw (1980), this will result in the polarization of sodic pyroxene compositions and may explain the apparent solvus in the sodic pyroxene field. Such a grouping is however not apparent in sodic pyroxene compositions from the glaucophane-lawsonite zone (cf., Okay 1980a, Fig. 4).

The sodic amphibole producing reaction in the Tavşanlı area can be balanced for the observed compositions of the participating minerals:

$$2.5\ Na_{0.80}Ca_{0.20}Al_{0.30}Fe^{3+}{}_{0.50}Mg_{0.16}Fe^{2+}{}_{0.04}Si_2O_6$$
sodic pyroxene

$$+0.5\ Mg_3Fe^{2+}{}_2Al_2Si_3O_8(OH)_8+2.5\ SiO_2=$$
chlorite quartz

$$0.5\ CaAl_2Si_2O_6(OH)_4$$
lawsonite

$$+1\ Na_2Mg_{1.90}Fe^{2+}{}_{1.10}Al_{0.75}Fe^{3+}{}_{1.25}Si_8O_{22}(OH)_2.$$
sodic amphibole

It is important to note that this reaction does not involve H_2O, and is thus independent of changes in fluid pressure.

The chlorite composition in the reaction is slightly idealised [$(Mg, Fe)_5Al_2$.... instead of $(Mg, Fe)_{4.8}$-$Al_{2.2}$...] and the small Ca-component in sodic amphibole is neglected in order to use the tabulated thermodynamic values. Entropies and molal volumes of sodic pyroxene, chlorite and sodic amphibole are obtained from their respective end-members (Helgeson et al. 1978) by assuming ideal mixing on sites. Ordering of ions in the M1 and M2 sites has been demonstrated for P lattice omphacites (Clark and Papike 1968). Aegirine-jadeites and chloromelanites, on the other hand, show no ordering and have the higher symmetry space group C2/c with equivalent M2 sites (Carpenter 1980). Therefore entropies of mixing for sodic pyroxenes and sodic amphiboles have been calculated assuming no coupling on sites. The entropy data ferroglaucophane is not available. It is assumed that increase in entropy from magnesioriebeckite to riebeckite (due to Mg $<=\Rightarrow$ Fe^{2+} substitution) is the same (18.6 cal/mol.K) as from glaucophane to ferroglaucophane, and a corresponding value for ferroglaucophane has been obtained (148.6 cal/mol. K).

There is a very small decrease in volume ($\Delta V=-1.45\ cm^3$; a decrease of 0.5% in volume compared with 17% for the reaction albite-> jadeite+quartz) and in entropy ($\Delta S=\sim -9$ cal/degree; a decrease of 4.7%) to the right side of the reaction. Such small changes in volume and entropy, well within the uncertainty of tabulated thermodynamic values and the assumptions involved, make the calculated slope of the reaction (dP/dT) meaningless.

Importance of Topotaxy in Low-Grade Metamorphism

Such small differences in ΔV and ΔS in low-grade metamorphism are unlikely to have been the determining factors in the formation of any new mineral assemblages. In low-grade (200°–300° C) static metamorphism, where there is no differential stress, nucleation of new minerals is difficult. One way of overcoming this problem of nucleation is by topotactic replacement of a preexisting mineral structure. In such circumstances a mineral assemblage could form, which, although not representing the lowest possible free energy of the system at the particular pressure and temperature, is kinetically favoured. Equilibrium may only be slowly attained (if at all) by a series of metastable mineral assemblages involving a sequence of "Oswald steps".

The important topotactic reaction in the Tavşanlı area is "sodic pyroxene pseudomorphing augite". It is clear that all sodic pyroxene in metabasites, both in the lawsonite and glaucophane-lawsonite zones, has formed initially as pseudomorphs after augite. Rocks with an already existing calcic amphibole (for example some rare basic alkali rocks with magmatic kaersutite) have developed a blue amphibole in a replacement texture. In such rocks a sodic pyroxene-chlorite assemblage was never formed.

In the formation of sodic amphibole, penetrative deformation has played an important role in facilitating the nucleation of new minerals. In fact the sodic amphibole isograd in Fig. 5 corresponds roughly to the limits of penetrative deformation in the metabasic rocks. In the more massive metadolerites of the glaucophane-lawsonite zone, sodic pyroxene pseudomorphs are clearly discernable, whereas in the surrounding more fissile tuffs they have been completely obliterated. This, and the common presence of the reaction mineral assemblage sodic amphibole + sodic pyroxene + chlorite + lawsonite + quartz in many glaucophane-lawsonite metabasites (cf., Okay 1980a Tables 1 and 2), indicates that all metabasites in the glaucophane-lawsonite zone have passed through a lawsonite zone stage.

The Type II and III metabasites of the Franciscan (Coleman and Lee 1963) are closely analogous both in mineralogy and texture to the lawsonite and glaucophane-lawsonite zone blueschists of Northwest Turkey. The presence of minor amounts of sodic amphibole in many Franciscan Type II metabasites (Coleman and Lee 1963; Brown and Bradshaw 1980, Table 2) indicates that most of the mineral assemblages are in fact reaction assemblages. The completion of the sodic amphibole producing reaction would be greatly facilitated by deformation and the characteristic feature of Type III metabasites is a strong penetrative fabric. The gradational contacts betweeen Type II and III metabasites in the Ward Creek area (Coleman and Lee 1963) may represent, like those in the Tavşanlı area, the limits of penetrative deformation.

The extensive presence of sodic pyroxene pseudomorphs after augite in many blueschist terrains of the world [in Franciscan Type II metabasites (Coleman and Lee 1963, p. 270; Ernst 1965, p. 888; Essene and Fyfe 1967, p. 3; Ernst et al. 1970, p. 49); in the lawsonite zone metabasites of New Caledonia (Black 1974, p. 282); in the Celebes, Indonesia (de Roever 1950, p. 1457); in the lawsonite-albite facies rocks of the Fuscaldo area in Italy (de Roever 1972, p. 63); in the Western Alps (Bearth 1965, p. 181) and in Corsican blueschist terrain (Brouwer and Egeler 1952, p. 32)] indicates that the reaction between sodic pyroxene and chlorite is an important sodic amphibole producing reaction in such rocks.

Several other reactions have been proposed for the formation of sodic amphibole in low-grade rocks. The often quoted sodic amphibole producing reaction (Miyashiro and Banno 1958, p. 101; de Roever and Beunk 1976, p. 224) of

albite + antigorite mol. in chlorite
= glaucophane + H_2O

is not realistic as there is no appreciable compositional difference between the lawsonite and glaucophane-lawsonite zone chlorites, and furthermore the actual sodic amphibole produced is generally a crossite rather than glaucophane. Sodic amphibole forming reactions involving calcite (Ernst 1963, p. 23) imply regional decarbonation for which there is no evidence at these low temperatures of metamorphism. As paragonite and stilpnomelane are both rare minerals in low-grade blueschists, sodic amphibole producing reactions involving these minerals (Ernst 1963, p. 23; Brown 1974, p. 339) would at the very best be of localised importance.

However, in the case of greenstones with the initial mineral assemblage of chlorite + albite + actinolite, sodic amphibole production can involve a one step reaction such as:

actinolite + chlorite + albite
= sodic amphibole + lawsonite,

This reaction (de Roever 1955, p. 241) is observed in the metabasites of the Panoche Pass, California (Ernst 1965, Fig. 2) and also in uralitised metagabbros in the Tavşanlı area (Okay 1980c).

It is not clear what niche in the P-T-X space the assemblage sodic pyroxene + chlorite + lawsonite + quartz occupies. It is quite plausible that in the Tavşanlı metabasites this assemblage may have formed metastably within the sodic amphibole + lawsonite stability field through the seeding effect of a preexisting pyroxene structure. If the initial spilitisation process had produced an assemblage of actinolite + albite + chlorite, this intermediate sodic pyroxene stage probably would not have been observed. This strong influence of the initial mineral assemblage on the reaction path suggests that reaction kinetics rather than the drive of the system towards the lowest free energy may be the dominant factor in the formation of new mineral assemblages in such low-grade metamorphic rocks.

Acknowledgements. I thank T.J.B. Holland, R. Muir Wood, and I. Rossol for reviewing the manuscript. This work was carried out while in receipt of a grant from the Mineral Research and Exploration Institute of Turkey (M.T.A.), which is gratefully acknowledged.

References

Bearth P (1965) Zur Entstehung alpinotyper Eklogite. Schweiz Mineral Petrogr Mitt 45:179–188

Black PM (1974) Mineralogy of New Caledonian metamorphic rocks III. Pyroxenes. Contrib Mineral Petrol 45:281–288

Brouwer HA, Egeler CG (1952) The glaucophane facies metamorphism in the Schistes Lustres Nappe of Corsica. Verh K Ned Akad Wet 48:1–71

Brown EH (1974) Comparison of the mineralogy and phase relations of blueschists from the North Cascades, Washington and greenschists from Otago, New Zealand. Bull Geol Soc Am 85:333–344

Brown EH, Bradshaw JY (1980) Phase relations of pyroxene and amphibole in greenstone, blueschist and eclogite of the Franciscan Complex, California. Contrib Mineral Petrol 71:67–83

Carpenter MA (1980) Mechanisms of exsolution in sodic pyroxenes. Contrib Mineral Petrol 71:289–300

Carpenter MA, Okay AI (1978) Topotactic replacement of augite by sodic pyroxene in a blueschist rock from NW Turkey. Mineral Mag 422:435–438

Clark JR, Papike JJ (1968) Crystal chemical characterization of omphacites. Am Mineral 53:840–867

Çoğulu E (1967) Etude pétrographique de la région de Mihaliççik (Turquie). Schweiz Mineral Petrogr Mitt 47:683–824

Coleman RG, Lee DE (1963) Glaucophane-bearing metamorphic rock types of the Cazadero area, California. J Petrol 4:260–301

Ernst WG (1963) Petrogenesis of glaucophane schists. J Petrol 4:1–30

Ernst WG (1965) Mineral paragenesis in Franciscan metamorphic rocks, Panoche Pass, California. Geol Soc Am Bull 76:879–914

Ernst WG, Seki Y, Onuki H, Gilbert MC (1970) Comparative study of low-grade metamorphism in the California Coast Ranges and the outer metamorphic belt of Japan. Geol Soc Am, Mem 124:259

Essene EJ, Fyfe WS (1967) Omphacite in Californian metamorphic rocks. Contrib Mineral Petrol 15:1–23

Greenwood HJ (1975) Thermodynamically valid projections of extensive phase relationships. Am Mineral 60:1–8

Helgeson HC, Delany JM, Nesbitt HW, Bird DK (1978) Summary and critique of the thermodynamic properties of rock forming minerals. Am J Sci 278A:1–299

Miyashiro A, Banno S (1958) Nature of glaucophanitic metamorphism. Am J Sci 256:97–110

Okay AI (1978) Sodic pyroxenes from metabasites in the eastern Mediterranean. Contrib Mineral Petrol 68:7–11

Okay AI (1980a) Mineralogy, petrology and phase relations of glaucophane-lawsonite zone blueschists from the Tavşanlı Region, Northwest Turkey. Contrib Mineral Petrol 72:243–255

Okay AI (1980b) Sodic amphiboles as oxygen fugacity indicators in metamorphism. J Geol 88:225–232

Okay AI (1980c) The petrology of blueschists in Northwest Turkey, Northeast of Tavşanlı. Ph D Thesis (unpubl). University of Cambridge

Roever EWF de (1972) Lawsonite-albite facies metamorphism near Fuscaldo, Calabria (Italy), its geological significance and petrological aspects. GUA Papers of Geology. Ser 1, no 3, 163 p

Roever EWF de, Beunk F (1976) Blue amphibole-albite-chlorite assemblage from Fuscaldo (S Italy) and the role of glaucophane in metamorphism. Contrib Mineral Petrol 58:221–234

Roever WP de (1950) Preliminary notes on glaucophane-bearing and other crystalline schists from South East Celebes, and on the origin of glaucophane-bearing rocks. K Ned Akad Wet 53:2–12

Roever WP de (1955) Some remarks concerning the origin of glaucophane in the North Berkeley Hills, California. Am J Sci 253:240–244

Sweatman RR, Long JVP (1969) Quantitative electron probe microanalysis of rock forming minerals. J Petrol 10:332–379

Whittaker EJW, Zussman J (1956) The characterization of serpentine minerals by X-ray diffraction. Mineral Mag 31:107–125

Accepted September 23, 1980